THE COLLEGE OF WILLIAM & MARY

Characterization of Optical Tweezers

Author:
Zachary Lutzky

Advisor:
Professor Bjorg Larson

Second Reader:
Professor Todd Averett

A thesis report submitted in fulfillment of the requirements for the degree of Physics From the College of William and Mary

in the

Professor Larson's Optical Tweezers Lab
William & Mary Physics Department

Williamsburg, VA
May 14, 2024

THE COLLEGE OF WILLIAM & MARY

Abstract

William & Mary Physics Department

Bachelor of Science

Characterization of Optical Tweezers

by Zachary Lutzky

This thesis discusses the construction and characterization of William & Mary's only operational optical tweezers. During the spring semester of 2023 and fall semester of 2024, the construction of the Modular Optical Tweezers was completed. During the spring semester of 2024, preparations for characterizing the optical tweezers were completed. These preparations included installing software, connecting the optical tweezers to the computer system, testing the quadrant photodetector (QPD), and aligning the optical elements of the system. This semester, the voltage-to-position calibration for the QPD was completed. Using the QPD, the trap stiffness was determined to be $1.5 \times 10^{-18} \pm 1.187 \times 10^{-20}$ N/m.

Acknowledgements

I would like to thank Professor Bjorg Larson for her help and contributions in setting up this research group. I have learned so much from you and I am forever grateful for your help. I also would like to thank Russel Burns (EPAD, 2025) for his contribution to the code to collect data. I am thankful for the amount of time he saved me. To Professor Todd Averett, thank you for being my second reader and for your suggested edits to my thesis. Thanks to Libby McClough (Biology and Math, 2026) and Aman Makonnen (Neuroscience, 2023) for helping with the construction of the optical tweezers. This project was funded by the William & Mary Faculty Research Committee Grant fund and the Higher Education Equipment Trust Fund.

Contents

List of Figures

Chapter 1

Background

1.1 What are Optical Tweezers?

Optical tweezers, or a single-beam gradient force trap, is a laser light technology that was pioneered by Dr. Arthur Ashkin in 1986 when he was able to trap polystyrene spheres using a laser focused through a microscope[1]. Optical tweezers are a scientific instrument that uses a highly focused laser beam to hold and move objects that range in size from atoms and nanoparticles to bacteria and droplets.

1.2 How do Optical Tweezers Work?

Optical tweezers work by using the idea that light carries momentum proportional to its energy and propagation direction. When a photon hits a particle there is an equal and opposite force to counteract the force applied. These forces in the trap are the gradient force and the scattering force as seen in Figure 1.1. Due to the fact that the optical setup is using ray optics and the applications and testing being done on the optical tweezers are using particles with a diameter $\leq 0.2\lambda_{trap} = 0.2 \times 976\text{nm} = 195.2$ nm (where λ_{trap} is the wavelength of the trapping beam), we will only be considering the Rayleigh regime and not the Mie regime where the diameter of particles $d >> \lambda$.

1.2.1 Scattering Force

The scattering force is produced by the photons striking the surface of the specimen, causing the specimen to move toward the direction of beam propagation. This force tends to push the specimen out of the trap, but by being balanced with the gradient force, stability is achieved. The scattering force equation is:

$$F_{scat} = \frac{I_0}{c}\frac{128\pi^5 r^6}{3\lambda^4}\left(\frac{m^2-1}{m^2+2}\right)^2 n_b \tag{1.1}$$

where F_{scat} = scattering force, I_0 = intensity, c = speed of light, r = radius of the target that is being trapped, λ = wavelength in medium, m = relative refractive index of the target and medium = $\frac{n_{bead}}{n_{medium}}$, and n_b = refractive index of the target

1.2.2 Gradient Force

The gradient force comes from the Gaussian intensity profile of the laser beam, causing the intensity to decrease as one gets farther from the center of the beam. This causes a restoring force, where particles are funneled toward the center of the beam.

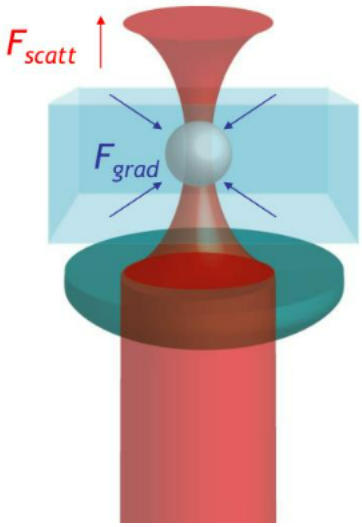

FIGURE 1.1: A force diagram showing the scattering force and the gradient force acting upon the particle[2].

The gradient force equation is:

$$F_{grad} = \frac{n_b r^3}{2}\left(\frac{m^2-1}{m^2-2}\right)\nabla E^2 \tag{1.2}$$

where F_{grad}= Gradient Force and ∇E = energy gradient

1.2.3 The Ratio of the Backward Axial Gradient Force to the Forward-Scattering Force

The ratio of the backward axial gradient force to the forward-scattering force is used to ensure that the optical trap is stable. R needs to be larger than 1 and the unity at the position of the maximum axial intensity gradient. Stability is reliant on the dominance of the backward axial gradient force. To find R we use the equation[1]:

$$R = \frac{F_{grad}}{F_{scat}} = \frac{3\sqrt{3}}{64\pi^5}\frac{n_b^2}{\left(\frac{m^2-1}{m^2+2}\right)}\frac{\lambda^5}{r^3\omega_0^2} \geq 1 \tag{1.3}$$

where ω_0 = focal spot size.

1.2.4 Numerical Aperture

Numerical Aperture (NA) is the characterization of the range of angles (θ) that a system can accept or emit light, with an index of refraction n_{medium}, with NA being determined by the equation:

$$NA = n_{medium}\sin\theta \tag{1.4}$$

In order for the ratio of the backward axial gradient force to the forward-scattering force to be greater than 1 we need to make the gradient force as large as possible. This

is why we need a high-NA oil immersion lens. This allows for $n = 1.5$ compared to an $n = 1$ for air or 1.33 for water[1].

1.3 Optical Trap Dynamics

A trapped particle experiences three forces that, when added together, equal zero. There is a Newtonian force which is usually gravity, a drag force from the medium, and a restoring force. In a system where a specimen, or in this case a bead, is suspended in a fluid a phenomenon known as Brownian motion occurs.

1.3.1 Brownian Motion

Brownian motion is caused by continuous and random collisions with solvent molecules, the solvent being the medium in which the particle is immersed in. This can be seen in the optical tweezers as all free-floating particles will be wiggling. It is highly dependent on temperature, with lower temperatures having fewer Brownian fluctuations. This is why having the optical tweezers in a temperature-controlled environment is key to accurate measurements[2].

1.3.2 Trap Stiffness

The optical trap behaves like a linear spring and that characteristic is reflected in the equation to calculate the stiffness of the trap, which is spring force:

$$F_{restoring} = kx \tag{1.5}$$

Where $F_{restoring}$ = restoring force, k=spring constant, and x=displacement. We can assume that our silica beads are spherical so we can use the Stokes drag force equation:

$$kx = 6\pi\eta rv \tag{1.6}$$

Where η=viscosity of the fluid medium and v = velocity in the fluid medium. To find the Stokes drag force we can measure the displacement of the trapped bead out of the trap due to the external drag force applied by the fluid flow[3]. Using the drag force we can also determine trapping force.

Chapter 2

Experimental Setup

2.1 ThorLabs Modular Optical Tweezers

The experimental setup that we have been working on to make optical tweezers is the THORLABS Modular Optical Tweezers as seen in Figure 2.1 [4]. In order to collect and analyze data and operate the system many programs were installed, which include: Matlab, Thorcam, Anaconda, Python coding software, kinesis software, optical power meter software, and LabVIEW. The kinesis software connects the computer to the sample positioning stage and the QPD. This allows for nanometer precision movement on the 3-axis stage. Piezo actuators move the stage by converting electrical energy into mechanical motion, based on the piezoelectric effect. This motion changes the electrical resistance in the strain gauge, which is converted to an electrical signal. This signal can be used for feedback compensation for the displacement of the piezo actuator. This setup allows for nanometer accuracy and is pointed out in 2.1 as the controllers for the stage. The setup uses a 976-nm trapping laser from a pigtailed fiber Bragg grating stabilized single-mode laser diode with an integrated thermoelectric cooler and thermister. It is collimated using a triplet fiber collimator[4]. The whole optical setup then went through several rounds of realignment.

2.2 Optical Setup

The optical setup is shown in Figure 2.2. A collimated 976-nm trapping laser beam is expanded to overfill the back aperture of the microscope objective lens. The first dichroic mirror (DM_1) reflects the infrared light to the 100X oil-immersion Nikon objective lens with an NA of 1.25 that focuses the light down to a spot size of 1.1 μm, which was calculated via $r = \frac{1.2\lambda}{NA}$[4]. The beam is subsequently concentrated into a diffraction-limited spot of high intensity within the sample chamber for the purpose of trapping. While the DM_1 and DM_2 reflect the infrared trapping beam, they transmit the visible spectrum white light that comes from the LED illumination source, allowing the white light to pass through the chamber, illuminate the sample, and go to the CCD camera. The CCD camera can then display real-time footage of the trapped specimen on the chamber plane. The condenser lens collects the forward scattered infrared light from the trapped particle, which reflects off of DM_2 and projects an image onto the quadrant photodetector (QPD) [5].

2.3 Quadrant Photodetector

The quadrant photodetector (QPD) allows for accurate photodetection, which gives precise measurements of the motion of the trapped particles. This is done by the

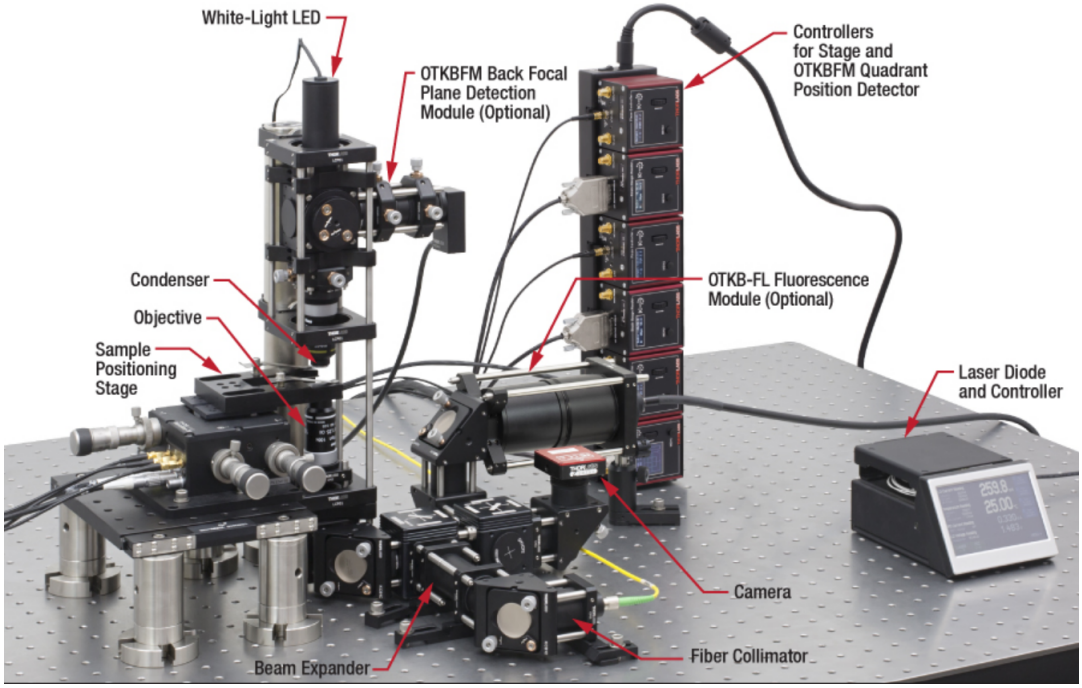

FIGURE 2.1: A photo by Thorlabs depicting their modular optical tweezers setup. Currently, we do not have the OTKB-FL Fluorescence module attached, due to it needing to be specialized for a sample type. Once we know what type of samples/materials we would want fluorescent we can acquire the needed light sources and install the OTKB-FL module.[4].

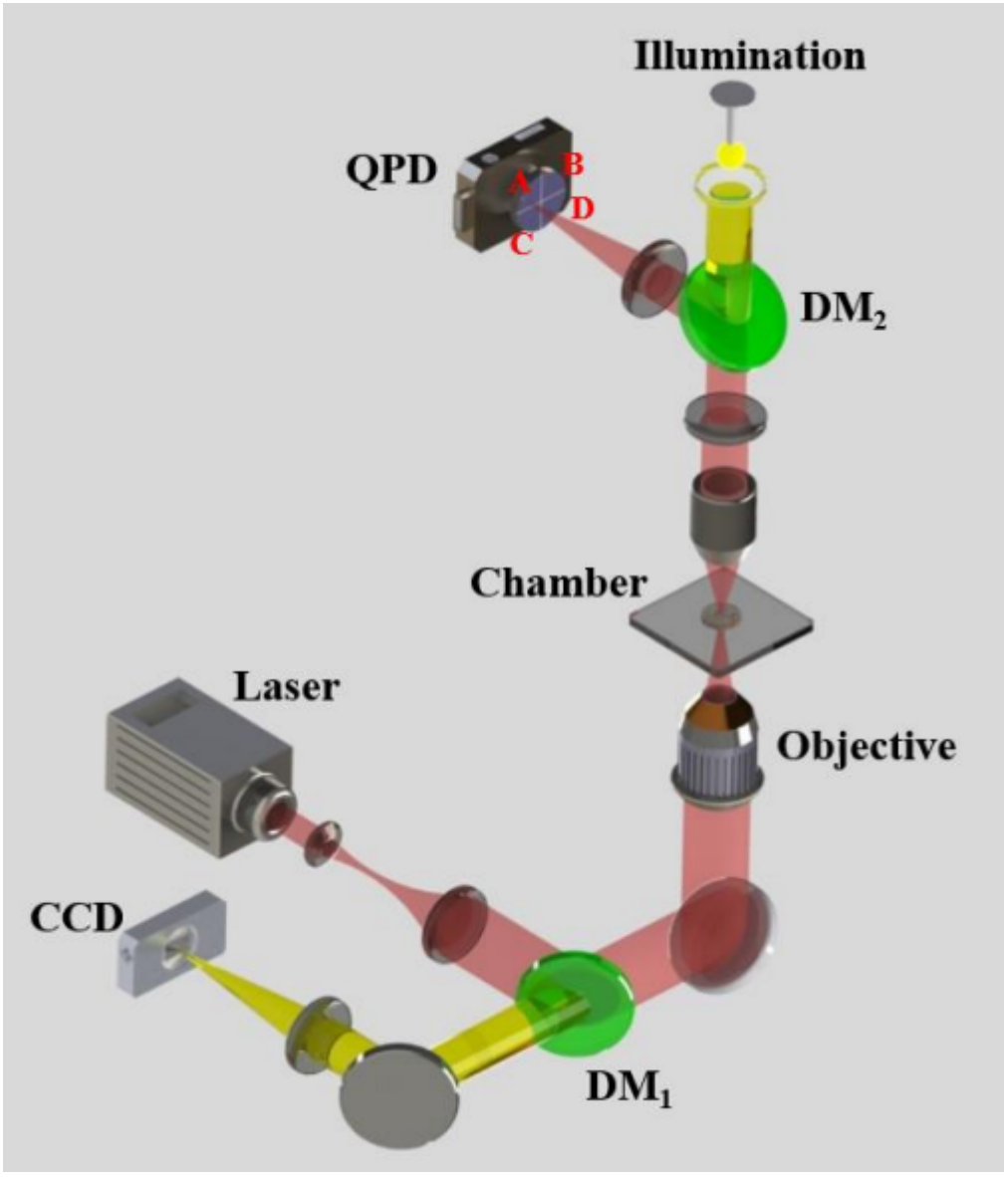

FIGURE 2.2: A diagram showing the optical setup for an optical tweezers assembly with a quadrant photodetector (QPD), a charged-coupled device (CCD), and two dichroic mirrors (DM) [5].

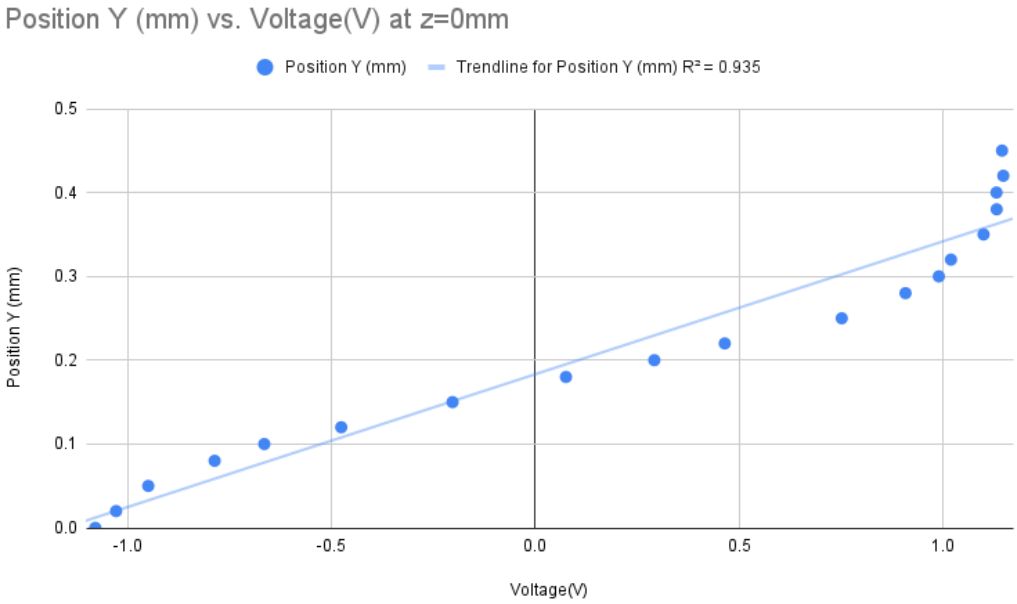

FIGURE 2.3: A graph showing the Y-axis position of the 633-nm helium-neon laser beam as it goes from the bottom of the quadrant photodetector to the top. The beam diameter is under 1 mm as it was at the focal point of the 50-mm lens. Out of the three beam diameters, this one had the lowest R^2 value of 0.935

four active photodiode areas arranged in a quadrant formation, with each quadrant generating a photocurrent proportional to the amount of light detected. By comparing the relative intensities of the photocurrents, the position of the trapped particles can be determined. The detection error or resolution of the QPD depends on the power level of the beam, but at its maximum power level is 0.75 microns.[4][5].

2.3.1 Testing Quadrant Photodetector

In order to test the quadrant photodetector and roughly determine the beam size that produces the most stable measurement, a 633-nm helium-neon laser, a 50-mm aspherical lens, a 0.11-ND filter, and a high-precision XYZ stage are used. By positioning the 633-nm helium-neon laser so that it is perpendicular to the lens, ND filter, and quadrant photodetector a setup that focuses the beam onto the quadrant photodetector can be made. The ND filter is necessary because it prevents the intensity of the laser from being higher than the maximum power of the quadrant photodetector. For the 633-nm laser the P_{max}=0.5 mW and the P_{min}=0.061 mW. For the 976-nm laser the P_{max}=0.308 mW and the P_{min}=0.0375 mW. By moving the quadrant photodetector towards the laser the beam profile can enlarged from under 1 mm to 1.5 mm to 3 mm. The results of the graphs can be seen in Figures 2.3, 2.4, 2.5. These graphs show that the desired beam diameter is around 2-3 mm as they had the highest R^2 values. The R^2 values can range from 0 to 1 and quantifies how well the data fits the linear regression model. Having a beam diameter around 2-3 mm results in less variance in the data and a higher degree of accuracy. This technique of measuring the beam crossing over the sensor in one axis will be used at a higher level of precision for the position calibration. This will be explained in 3.1.1.

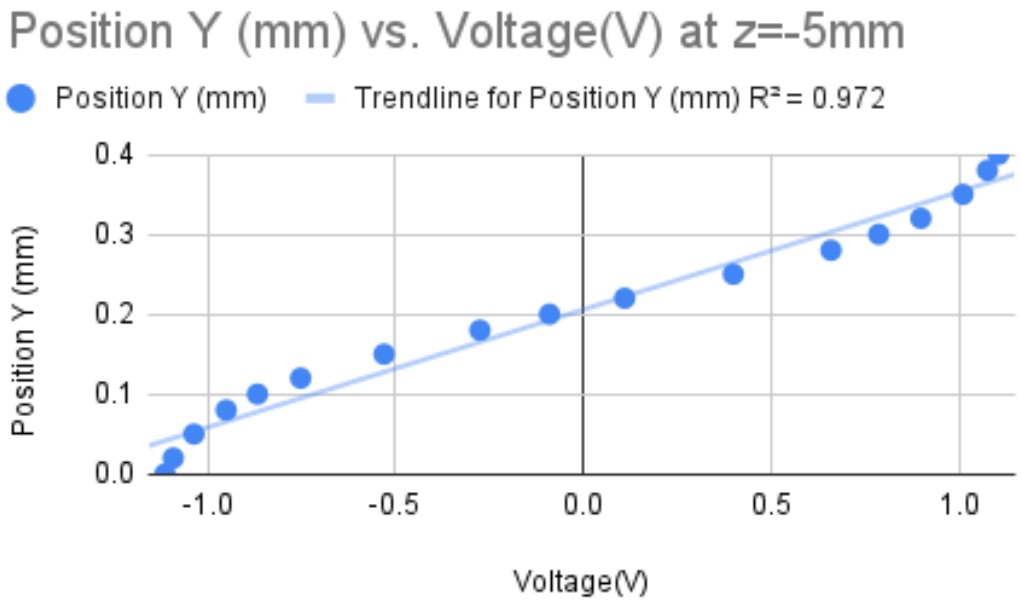

FIGURE 2.4: A graph showing the Y-axis position of the 633-nm helium-neon laser beam as it goes from the bottom of the quadrant photodetector to the top. The beam diameter is 1.5 mm and was moved 5 mm away from the focal point of the 50-mm lens. The R^2 value of 0.972 is desirable due to it being closer to 1

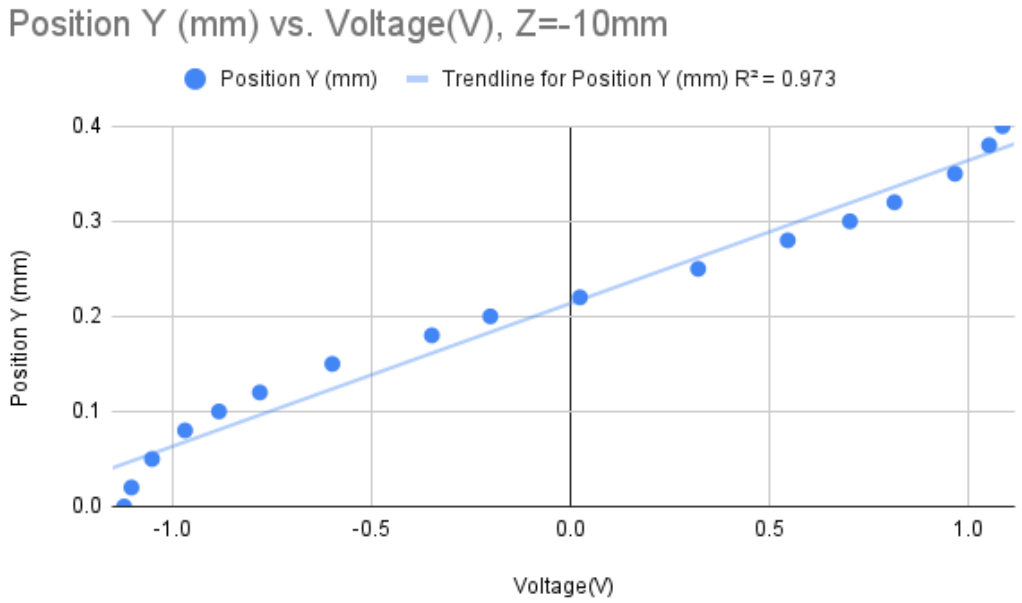

FIGURE 2.5: A graph showing the Y-axis position of the 633-nm helium-neon laser beam as it goes from the bottom of the quadrant photodetector to the top. The beam diameter is 3 mm and was moved 10 mm away from the focal point of the 50-mm lens. The R^2 value of 0.973 is desirable due to it being closer to 1

Chapter 3

Trap Stiffness

3.1 Characterization

The optical tweezers need to be characterized so that it can be properly utilized by other research groups for future work. Once factors like trap stiffness and minimum and maximum trapping size, it will be easier to judge what projects our optical tweezers can contribute to.

3.1.1 Position Calibration

The position calibration involves taking an immobilized bead on a slide and moving it in increments of 0.05 microns in the X and Y axis while recording the corresponding voltages from the QPD. From this data, a linear voltage to displacement calibration factor ρ can be made, which will be used for the following trap stiffness calibrations. ρ is made by fitting a linear regression model of $y = ax + b$ to the scan of the bead in a single axis, which can be seen in Figure 3.1. ρ changes with laser power so we will need to find ρ for any laser currents that we may need. 50 mA is the lowest level that we can successfully trap at and 120 mA is the highest current we can have before the optical power outputted is outside the range of the QPD. The linear fit for the currents can be found in Table 3.1. A graph of the slopes can be found in Figure 3.2. The QPD's sensitivity depends on two factors, the wavelength of light hitting it and the optical power of that light. The 976 nm wavelength is near the peak of sesitivity of the QPD. This means that laser current will determine how sensitive the QPD is. This can be seen in Figure 3.2 as both the error and the divergence of the X and Y axis slopes increases with current.

3.2 Trap Stiffness Calibration

Trap stiffness can be evaluated in several ways, but there are three that can be done for our system. Due to the data acquisition card (DAQ) not being ready for operation trap stiffness was found via the equipartition theorem. The DAQ card has an acquisition rate greater than 10 kHz and is needed to do Stokes drag calibration and Lorentzian profile of the power spectrum.

3.2.1 Equipartition Theorem

The equipartition theorem states that each degree of freedom in a harmonic potential has $k_B T/2$ of energy. We can use this to relate the measurement of the instantaneous

displacement of a trapped particle to the available thermal energy of a system defined by the equation[3];

$$\frac{1}{2}k_B T = \frac{1}{2}\langle (R - R_{mean})^2 \rangle k \tag{3.1}$$

Where $R = \sqrt{x^2 + y^2}$, k_B= Boltzmann constant and T =temperature. Due to limited resources and time, the temperature of the system was determined via the infrared emission from the glass well that held the trapped beads. The temperature of the well was determined to be 296.5 ± 0.7 K, with the temperature being taken repeatedly over two hours. In order to ensure the least temperature deviation was kept to a minimum, the diluted bead solution was left outside the storage fridge for 24 hours and then left with the trapping beam on for a further two hours to account for deviation due to the laser heating up the solution. To see the kinetic energy of the bead due to temperature while it is trapped we need it to be very weakly trapped for this method to work. This means that a limitation of this measurement method is that it can not measure the stiffness at higher trapping powers because the movement due to Brownian motion is smaller than the resolution of our sensor and is in the nanometer and sub-nanometer scale. We will need to find trap stiffness using the other two methods previously mentioned to determine stiffness at higher power levels. To find the trap stiffness using the equipartition theorem we trapped the bead at 50 mA, which was just strong enough to keep the bead trapped. The QPD then took over a hundred data points over the course of two minutes in order to see how much the bead moved while trapped. We then take the X-axis and Y-axis data sets and using equation $R = \sqrt{x^2 + y^2}$, we calculate the magnitude R by squaring the X and Y values and taking the square root of their sum. Next, we find the mean of the R data set. By subtracting this mean from all points in the R data set, we create a new data set. We then square the values in this new data set and calculate their average. Finally, we plug this average into equation 3.1. The trap stiffness was determined to be $1.5 \times 10^{-18} \pm 1.187 \times 10^{-20}$ N/m.

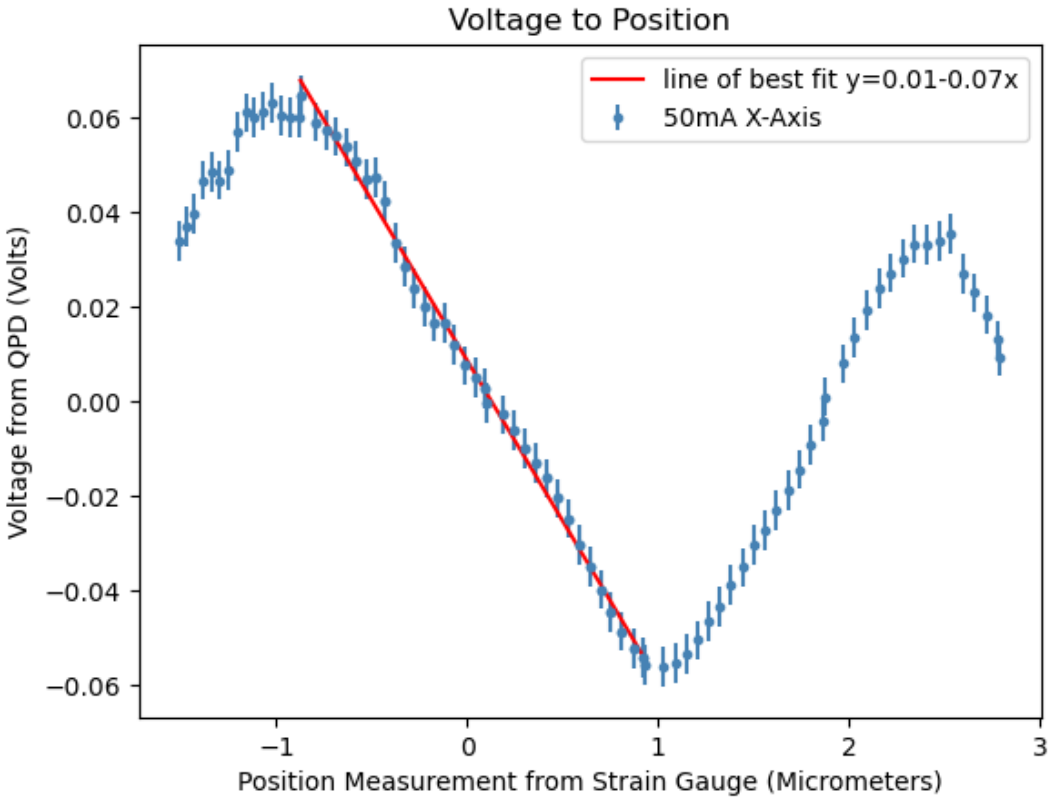

FIGURE 3.1: A Graph showing the X-axis position of the 976-nm trapping laser beam as it scans a fused silica bead. The position of the bead determined by the QPD is read as a voltage and the change in position in microns read by the strain gauge reader. Using this graph we can determine the translation of voltage to position by making a linear fit. Error bars are ±0.00416 volts. Line of best fit is centered around the middle of the bead, which is read as zero volts. The linear fit (y=ax+b) is y=-0.07x+ 0.01, with uncertainty for a is ±0.000427 and b having ±0.00079.

TABLE 3.1: Linear Fits at Different Laser Currents

Linear Fit equation; y=ax+b			
Laser Current and Axis Scanned	Linear Fit	Uncertainty for a	Uncertainty for b
50 mA x-axis	y=-0.07x+0.01	±0.00079	±0.000427
50 mA y-axis	y=-0.07x+0.0	±0.00079	±0.00044
60 mA x-axis	y=-0.18x+0.29	±0.001315	±0.0022
60 mA y-axis	y=-0.18x+0.32	±0.00207	±0.003422
80 mA x-axis	y=-0.38x+0.63	±0.0054	±0.008457
80 mA y-axis	y=-0.40x+0.48	±0.00436	±0.00489
100 mA x-axis	y=-0.60x+0.78	±0.00787	±0.00981
100 mA y-axis	y=-0.65x+0.85	±0.006431	±0.008203
120 mA x-axis	y=-0.86x+2.30	±0.0113	±0.0297
120 mA y-axis	y=-0.89x+1.89	±0.01644	±0.02137

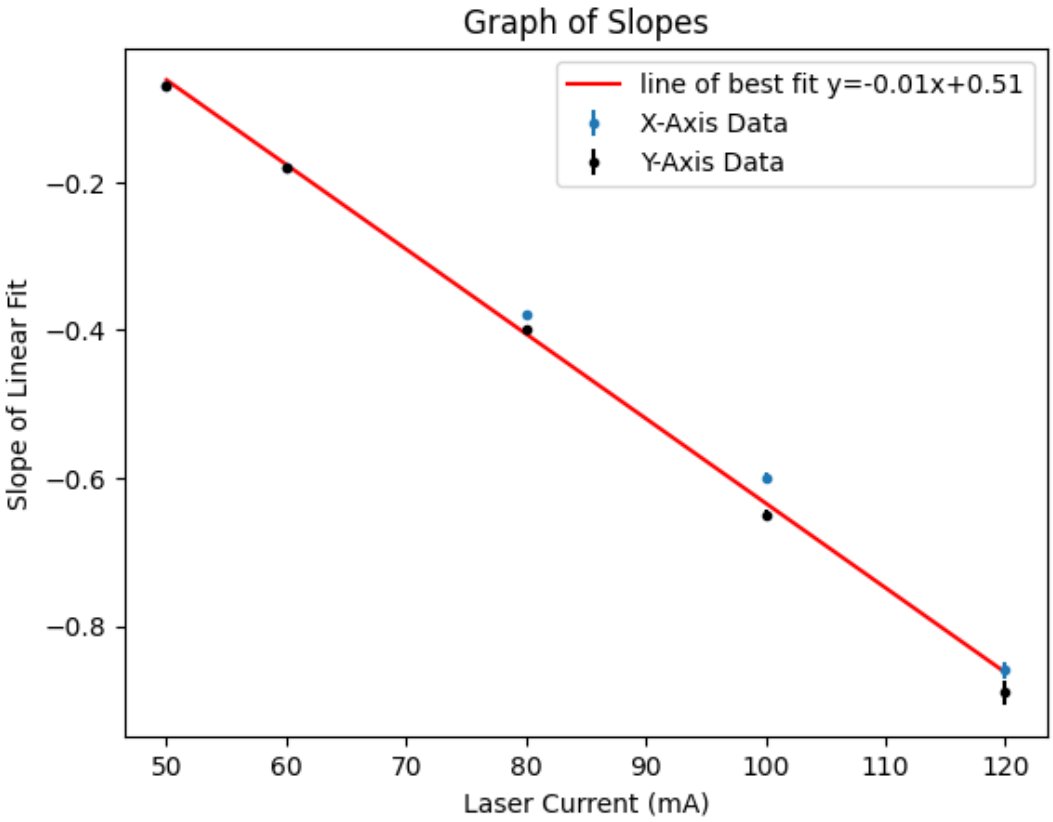

FIGURE 3.2: A Graph showing the slopes of the linear fits at different laser currents. The sensitivity of the QPD increases with optical power, so at higher laser currents the X and Y slope and more error. The linear fit (y=ax+b) is y=-0.01x+ 0.51. We can use this fit to predict the ρ at different currents.

3.2.2 Stokes Drag Calibration

The Stokes drag calibration method measures the displacement of a trapped bead out of the center of the trap caused by an external drag force that is applied when the trapped bead creates a laminar drag flow at a controlled velocity. We know the drag force from equations 1.5 and 1.6. Using the piezo actuators we can displace the bead at a controlled displacement and velocity and calculate the drag force coefficient[3].

3.2.3 Lorentzian Profile of the Power Spectrum

Using the thermal motion of the trapped bead and the Lorentzian profile of the power spectrum equation,

$$S_{VV}(f) = \rho^2 \frac{k_B T}{\pi^2 \beta (f_0^2 + f^2)} \tag{3.2}$$

where S_{VV} = uncalibrated power spectrum, f =frequency, f_0 = corner frequency, and β = drag coefficient = $6\pi\eta r$. By finding the roll-off or corner frequency (f_0) we can find the trap stiffness using;

$$k = f_0 2\pi\beta \tag{3.3}$$

This method has the advantage of being independent of the detector voltage to displacement[3].

3.3 Possible Modifications

A possible modification that can be easily added is an oscillating optical trap. An oscillating optical trap has the focal point moving up and down in the Z-axis, allowing rod-shaped bacteria to be aligned with their long axis lying within the focal plane. Oscillating optical traps are advantageous when it comes to imaging rod-shaped objects and increasing the tolerable infrared exposure dosage, but come at the expense of image resolution[6].

3.4 In Conclusion

In summary, this thesis focused on the construction and characterization of William & Mary's sole operational optical tweezers. Over the course of the spring semester in 2022 and the fall semester in 2023, the Modular Optical Tweezers were successfully built. Subsequently, during the spring semester of 2024, meticulous preparations were made for characterizing the optical tweezers. These preparations encompassed software installation, system connection, QPD testing, and optical element alignment. Now the voltage-to-position calibration for the QPD has been completed, leading to the determination of a trap stiffness, via the equipartition theorem, of approximately $1.5 \times 10^{-18} \pm 1.187 \times 10^{-20}$ N/m using the QPD.

Bibliography

[1] A. Ashkin, J. M. Dziedzic, J. E. Bjorkholm, Steven Chu (1986). Observation of a single-beam gradient force optical trap for dielectric particles. Opt. Lett. 11, 288-290. DOI: 10.1364/ol.11.000288

[2] van Mameren, J., Wuite, G.J.L., Heller, I. (2018). Introduction to Optical Tweezers: Background, System Designs, and Commercial Solutions. In: Peterman, E. (eds) Single Molecule Analysis. Methods in Molecular Biology, vol 1665. Humana Press, New York, NY. https://doi.org/10.1007/978-1-4939-7271-5_1

[3] D. C. Appleyard, K. Y. Vandermeulen, H. Lee, M. J. Lang (2007). Optical trapping for undergraduates. Am. J. Phys. 1 January 2007; 75 (1): 5–14. https://doi.org/10.1119/1.2366734

[4] Thor Labs. "Modular Optical Tweezers." Thorlabs.De, www.thorlabs.de/newgrouppage9.cfm?objectgroup_id=3959. Accessed 4 Dec. 2023

[5] Woerdemann, M. (2012). Introduction to Optical Trapping. In: Structured Light Fields. Springer Theses. Springer, Berlin, Heidelberg. https://doi.org/10.1007/978-3-642-29323-8_2

[6] Zhang, Z., Kimkes, T.E.P., Heinemann, M. Manipulating rod-shaped bacteria with optical tweezers. Sci Rep 9, 19086 (2019). https://doi.org/10.1038/s41598-019-55657-y